Potent Inhibition of Terminal Complement Assembly by Clusterin: Characterization of Its Impact on C9 Polymerization[†]

John F. McDonald and Gary L. Nelsestuen*

Department of Biochemistry, University of Minnesota, St. Paul, Minnesota 55108

Received November 22, 1996; Revised Manuscript Received March 26, 1997[⊗]

ABSTRACT: The interactions of the heterodimeric apolipoprotein and complement inhibitor, clusterin (CL, 80 kDa), with actively assembling terminal complement proteins were characterized. Clusterin inhibited at three sites and by two modes of action. Clusterin inhibited C9 assembly on C5b-8 and C5b-9 and also bound to C5b-7 to prevent membrane attachment. The impact on C5b-9 assembly was the most potent. C9 assembly was monitored by assembly-induced fluorescence changes of C9 labeled with fluorescein isothiocyanate (FITC-C9). Assembly of monomeric FITC-C9 with C5b-8 or C5b-9_1 produced a substantial decrease in fluorescence intensity due to changes in the environment of the probe. Addition of the next subunit of unlabeled C9 produced a further small change. One equivalent of FITC-C9 bound to C5b-8 at low temperatures, but the fluorescence change and addition of more C9 did not occur until the temperaure was increased. Kinetic analysis of the fluorescence change suggested an irreversible, first-order process with an activation energy of 29 kcal/mol ($k = 0.12$ s^{-1} at 25 °C). The kinetic properties differed for C9 addition to C5b-9_1 (0.27 s^{-1} at 25 °C, 21 kcal/mol), indicating that C9 activation occurred at a different or altered site. Clusterin binding to C5b-8−$(FITC\text{-}C9)_1$ caused fluorescence quenching similar to that of unlabeled C9, indicating that it bound to the C9 binding site. Clusterin binding to C5b-8 and C5b-9_1 was reversible with affinities that were 2 and 15 times that of C9 for the C5b-8 and C5b-9_1 complexes, respectively. The results suggested that the presence of <10% of the circulating clusterin in its heterodimeric, active form could reduce the rate of complement cytolysis of nucleated cells by 10-fold, and under some conditions by 100-fold or more. This would provide a high level of protection for certain cells and may allow time for action by other inhibitors of complement.

Clusterin (CL)[1] is an 80 kDa heterodimeric glycoprotein which has been implicated in the regulation of several biological actions (Rosenberg & Silkensen, 1995). These include lipid transport (Jenne et al., 1991), cell adhesion (Silkenson et al., 1995), fertility (Murphy et al., 1989a,b), and complement regulation (Murphy et al., 1989a,b). Clusterin may also be induced or activated in response to a number of pathological states such as renal tubular injury (Rosenberg et al., 1993), myocardial infarction (Vakeva et al., 1993), and Alzheimer's disease (Ghiso et al., 1993). In most of these cases, the role of clusterin is unknown or speculative. Direct biological acitivity has been shown for cell aggregation (Silkenson et al., 1995) and complement inhibition (Murphy et al., 1989a,b). The former is thought to be related to a role for clusterin in promoting cell−cell interactions where tissue disruption has occurred. The role of clusterin in complement inhibition is supported by its presence in the soluble terminal complement complex formed by vitronectin and the proteins C5b, C6, C7, C8α−γ, C8β, and C9 (Murphy et al., 1988). Clusterin also inhibits hemolysis of erythrocytes by complement, *in vitro* (Murphy et al., 1989a,b).

Although clusterin has been shown to bind to complement proteins in their denatured states (Tschopp et al., 1993), its sites and mechansim of action as well as its relative potency in physiological situations have not been thoroughly defined. One problem is the lack of methods that distinguish interactions of individual terminal complement proteins rather than observation of the end product, cell lysis due to complement. Identification of specific sites of clusterin interaction may contribute to an understanding of complement regulation at the level of assembly of the membrane attack complex (MAC) and may suggest the nature of clusterin interactions with other biological materials.

This study found that the fluorescence of complement C9 labeled with fluorescein isothiocyanate (FITC-C9) could discriminate two stages of C9 assembly. This allowed the detailed analysis of events related to unimolecular C9 assembly rather than to overall polymerization. Clusterin interacted with the C9-binding site of C5b-8 and with C5b-9, reducing the rate of further C9 addition. The interaction was reversible and of high affinity. Clusterin would provide the most potent protection for cells whose lysis required several C9 molecules per MAC.

MATERIALS AND METHODS

Materials. Fluorescein 5-isothiocyanate (FITC, isomer 1) was obtained from Molecular Probes (Eugene, OR) and 5(6)-

[†] Supported in part by Grant HL15728 from the National Institutes of Health. John F. McDonald was supported by a training grant (GM07232) from the National Institutes of Health.

* Corresponding author: Gary L. Nelsestuen, Department of Biochemistry, 1479 Gortner Ave., St. Paul, MN 55108. Fax: (612) 625-5780. E-mail: gary-N@biosci.cbs.umn.edu. Phone: (612) 624-3622.

[⊗] Abstract published in *Advance ACS Abstracts,* June 1, 1997.

[1] Abbreviations: CL, clusterin; FITC, fluorescein 5-isothiocyanate; MAC, membrane attack complex; PC, phosphatidylcholine; PS, phosphatidylserine; SUV, small unilamellar vesicles; d:p, dye per protein; BSA, bovine serum albumin; BCA, bicinchoninic acid; CyC, cytolytic complexes; SDS−PAGE, sodium dodecyl sulfate−polyacrylamide gel electrophoresis.

S0006-2960(96)02895-4 CCC: $14.00

carboxyfluorescein from Kodak (Rochester, NY). Phosphatidylcholine (PC, 99% from egg yolk), phosphatidylserine (PS, 98% from bovine brain), and Triton X-100 were obtained from Sigma Chemical Co. (St. Louis, MO). Dimethylformamide was obtained from Pierce (Rockford, IL). All other resins, buffers, and solvents were obtained from Sigma Chemical Co. or Fischer Scientific (Pittsburgh, PA).

Proteins and Vesicles. Complement proteins C5b-6 (Podack et al., 1978), C7 (Silversmith & Nelsestuen, 1986), C8 (Steckel et al., 1980), and C9 (Biesecker & Mueller-Eberhard, 1980) were isolated from human cryo-poor plasma (Memorial Blood Center, Minneapolis, MN) according to described methods. Extinction coeffiecients at 280 nm used to calculate protein concentrations were as follows: 1.0 mL mg^{-1} cm^{-1} for C7 (Podack et al., 1979), 1.6 mL mg^{-1} cm^{-1} for C8, and 0.99 mL mg^{-1} cm^{-1} for C9 (Podack & Tschopp, 1982). The complement proteins were fully active in hemolysis, assayed under conditions described below. Human clusterin was obtained from Quidel Co. (San Diego, CA) as a lyophiized sample at >95% purity (supplier's estimate). The concentration was estimated by a molecular weight of 80 000 (Kirszbaum et al., 1989). It was stored at <4 °C in a solution of the standard buffer and was used within 2 weeks. Small unilamellar vesicles (SUV) were composed of 75% PC and 25% PS and were prepared at 7 mg/mL in 50 mM Tris-HCl (pH 7.5) containing 0.1 M NaCl and 0.02% NaN_3 (standard buffer), by sonication and gel filtration as previously described (Plager & Nelsestuen, 1994). The phospholipid concentration of the vesicles was determined by organic phosphate assay using a weight ratio of phospholipid:phosphorus of 25 (Chen et al., 1956). The average vesicle diameter was 30−40 nm as determined by quasi-elastic light scattering (Bloomfield & Lim, 1978) using a Langley Ford model LSA2 spectrophotometer coupled to a model 1096 autocorrelator. Small unilamellar vesicles containing 5(6)-carboxyfluorescein were prepared in a similar manner using 40 mg of PC in 3 mL of a solution containing 200 mM dye. The mixture was gel filtered on a column of Sepharose 4B, and fractions containing vesicles with a 50−100 nm diameter were collected. The vesicles were dialyzed against the standard buffer. They were stored under the same conditions and could be used for up to 1 week after preparation.

Fluorescent Labeling of C9. Labeling of complement C9 with FITC was carried out in 50 mM sodium bicarbonate/NaOH buffer (pH 9) containing 0.1 M NaCl. The dye was freshly prepared in dimethylformamide (10 mM) and delivered to a solution of protein (0.5−1.0 mg/mL), which was stirred at room temperature in the dark. Sequential additions were made, each containing a 5-fold molar excess of dye over protein. The solution was stirred for 20 min after each addition. The maximum dye used was a 15:1 ratio of dye to protein. Once the reaction was complete, the solution was chromatographed at 4 °C on a Sepharose S-300 HR column (30 cm × 0.9 cm) equilibrated in 50 mM Tris-HCl buffer containing 0.1 M NaCl in 5% glycerol and 1% Triton X-100. This step removed free dye and protein aggregates. Concentrations of labeled protein solutions were determined by BCA assay using bovine serum albumin (BSA) as the standard (Smith et al., 1985). The results agreed closely with protein concentrations determined by absorbance at 280 nm. The average number of dye molecules incorporated per protein (d:p) was calculated from protein and dye concentrations in the various preparations. Dye concentrations were determined from absorbance at 495 nm on the basis of its reported extinction coefficients ($\epsilon^{495} = 76\,000$ M^{-1} cm^{-1} for FITC; Haugland, 1992). The final ratio of covalent dye per protein (d:p) was 0.5−1.0. SDS−polyacrylamide gel electrophoresis (SDS−PAGE; Laemmli, 1970) was used to verify that the label was covalently bound to the protein. Samples of FITC-C9 were developed on a 10% polyacrylamide gel with a 1 mm thickness under nonreducing conditions. Following electrophoresis, the lane was divided into 18 equal sections which were incubated in 1 mL of standard buffer at 37 °C for 4 h. After centrifugation at 13 000*g*, the fluorescence intensity of the extracts was measured. For all samples, >80% of the fluorescence intensity was found in the gel slices that comigrated with C9 that was detected by Coomassie stain of a separate lane (66 kDa). The fluorescence intensity of material that did not enter the gel did not exceed 4% of the total. The labeled protein was stored at −70 °C in the column eluant buffer. The presence of Triton prevented protein aggregation which sometimes occurred during long-term storage of labeled protein. Full protein function was estimated by subsequent assembly of the MAC as described below, and its biological activity was verified by the hemolytic assay.

Light Scattering and Other Assays of MAC Assembly. Light scattering and fluorescence were used to measure MAC assembly at 25 °C in standard buffer and a volume of 0.5 mL. Rayleigh light scattering at 90° was used to quantitate the binding of proteins to small unilamellar vesicles according to the method of Nelsestuen and Lim (1977). The assembly procedure was similar to that described by Silversmith and Nelsestuen (1986a,b). Upon addition of successive protein components (C5b-6, C7, C8, and C9), assembly of the MAC was monitored by excess light scattering intensity resulting from association of proteins with phospholipid vesicles. The quantity of C7 and C8 added was sufficient to saturate the C5b-6 present, as measured by light scattering increases. Equation 1 describes the light scattering changes for assembly of protein on phospholipid vesicles whose diameters are small relative to the wavelength of incident light.

$$I_2/I_1 = (M_2/M_1)^2[(\delta n/\delta c_2)/(\delta n/\delta c_1)]^2 \qquad (1)$$

I_2 and I_1 are the light scattering intensities of the protein−vesicle complex and vesicles alone, respectively. The vesicle concentration was the same in both measurements. M_2 and M_1 are the weight-average molecular weights of the protein−vesicle complex and vesicles alone, respectively, and $\delta n/\delta c_2$ and $\delta n/\delta c_1$ are the refractive index increments for protein−vesicle complexes and vesicles, respectively. The refractive index increment was assumed to be equal to the weight-averaged composition of each particle with a $\delta n/\delta c$ of 0.19 for pure protein and 0.17 for phospholipid (Nelsestuen & Lim, 1977). All experiments with vesicles were conducted under conditions that gave quantitative protein assembly [described by Silversmith and Nelsestuen (1986b)]. Briefly, M_2/M_1 values in eq 1 were obtained for each assembled species: addition of C5b-7 to vesicles [$M_r^{(\text{ves-C5b-7})}/M_r^{(\text{ves})}$] and assembly of C5b-8 on vesicles [$M_r^{(\text{ves-C5b-8})}/M_r^{(\text{ves})}$] and of C5b-9 [$M_r^{(\text{ves-C5b-9})}/M_r^{(\text{ves})}$]. The molecular weight ratios for addition of individual proteins were obtained from eqs 2

and 3 (Silversmith & Nelsestuen, 1986b). The stoichiometries of the assembled proteins were calculated from the same equations and the molecular weights of the MAC components: C5b-6, 325 000; C7, 120 000 (Podack et al., 1978); C8, 150 000 (Steckel et al., 1980); and C9, 66 000 (Stanley & Herz, 1987). In most experiments, C5b-6 was the limiting component, and protein equivalents, when referred to in this paper, are based on this species. Its concentration was estimated from several relationships. The weight concentration of vesicles (C_{ves}) was determined by the phosphorus assay. Under excess C7, the concentration of vesicle-bound C5b-6 was obtained from eq 4, which effectively determines amounts of assembled C5b-7 from the vesicle concentration. The validity of eq 4 was tested by

$$M_{r(C5b-8)}/M_{r(C5b-7)} = [M_{r(ves-C5b-8)}/M_{r(ves)} - 1]/[M_{r(ves-C5b-7)}/M_{r(ves)} - 1] \quad (2)$$

$$M_{r(C5b-9)}/M_{r(C5b-8)} = [M_{r(ves-C5b-9)}/M_{r(ves)} - 1]/[M_{r(ves-C5b-8)}/M_{r(ves)} - 1] \quad (3)$$

$$C_{C5b-7} = [M_{r(ves-C5b-7)}/M_{r(ves)}](C_{ves}) - C_{ves} \quad (4)$$

experiments in which C7 was limiting. In this case, C_{C5b-7} was calculated from the amount of C7 added and C_{ves} from the phosphorus assay. The $M_{r(ves-C5b-7)}/M_{r(ves)}$ calculated in this manner agreed, within experimental limits of ±20%, with that determined by light scattering. A similar cross-check was made for C9 assembly on the basis of concentrations of added C9 versus C9 calculated from $M_{r(C5b-9)}/M_{r(ves)}$, with the latter result being independent of component concentrations. This determination was made for each lot of C5b-6 and gave similar levels of agreement with light scattering measurements (see Results). Replicate experiments by any single method showed a small standard deviation. Protein concentrations and stoichiometries obtained by several methods suggest a systemic error of ≤20%, and conclusions drawn are subject to this larger error limit. These assays were corroborated by the ability of MAC proteins to induce carboxyfluorescein release from dye-loaded vesicles as described by Silversmith and Nelsestuen (1986c). The concentration of the limiting component (C7 or C8) correlated closely with the release of dye from vesicles, assuming a vesicle M_r of 5×10^6. The amount of active C5b-6 or C7 agreed, within limits of ±20%, with that found by the light scattering assay.

Light scattering measurements were performed on the SPEX Fluoromax fluorometer (JY/SPEXinstrumentsSA. Inc., Edison, NJ) with excitation and emission set at 320 nm. Small corrections of intensity measurements were made for dilution and background scattering from buffer and unbound protein, and from Triton. Triton, present in the labeled protein preparation, interacted with the vesicles and caused a small increase in light scattering. For example, the excess light scattering arising from titration of FITC-C9 and vesicles which contained only C5b-7 was due to the impact of Triton since FITC-C9 did not add to the complex. This intensity was stable with less than 10% of the change arising from assembly of one FITC-C9. It was less than 5% of the change at 70% saturation.

Steady State Fluorescence. Steady state fluorescence intensity measurements and emission scans were performed on the SPEX Fluoromax fluorometer in the ratio mode using a reference photodiode signal. Measurements were carried out in 10 × 0.3 cm quartz cuvettes (NSG Precision Cells, Inc., Farmingdale, NY) at 25 °C. Scans were conducted several times with intermittent mixing of the sample to confirm the stability of the signal. FITC fluorescence was measured with excitation and emission at 490 and 518 nm, respectively. Emission scans were obtained (excitation at 490 nm) from 500 to 650 nm. All measurements were corrected for dilution and the background from the buffer.

The fluorescence emission of 5(6)-carboxyfluorescein was measured with excitation and emission at 495 and 518 nm, respectively. Vesicles loaded with this dye had relatively low fluorescence intensities due to self-quenching of the dye at the high concentrations inside the vesicles. Measurements were recorded as the change in fluorescence intensity resulting from addition of the limiting complement protein to vesicle solutions containing the other MAC proteins.

Stopped-Flow Measurements. Stopped-flow measurements of FITC-C9 fluorescence were carried out with the SLM 4800C fluorometer (SLM-Aminco, Urbana, IL) equipped with a Milli-Flow Stopped Flow Reactor. The excitation wavelength was set at 495 nm by the instrument monochromator, and the emission wavelength was selected by a 520 ± 5 nm band-pass filter. Reactions were run at 25 °C and initiated by advancing the drive syringes with nitrogen pressure (70 psi) through a 2 μL mixing channel into an observation chamber. Data points were collected at 0.05−0.1 s intervals, averaged from the sum of 1 ms readings. Three to five experiments were averaged to provide the data shown. The dead time for the instrument was estimated to be 7 ms by the fluorescence reaction of pyranine with bovine carbonic anhydrase as described by the maufacturer. This was less than 10% of the half-time for the fluorescence changes measured in this study. Small, nonspecific changes in fluoresence intensity (<4%) were prevented by addition of 1 mg/mL BSA to the labeled protein solution. In the absence of BSA, these small changes were measured in control experiments and subtracted as a background. The presence of BSA had no detected impact on FITC-C9 assembly kinetics.

Other Methods. Protein concentrations were determined using the Bradford assay (Bradford, 1976) and by 280 nm absorbance using the published extinction coefficients. These methods gave comparable protein concentrations (<20% divergence). Hemolytic activity was measured according to procedures described previously (Kabat & Mayer, 1961) to verify that isolated proteins were physiologically active. Hemolytic assays were carried out in 0.5 mL of gel veronal buffer containing sensitized sheep red blood cells (2 × 108 cells/mL, Sigma Chemical Co.), C5b-6 (0.31 nM), C7 (0.11 nM), C8 (0.27 nM), and C9 (0.21 nM). Samples were incubated for 15 min at 37 °C and centrifuged, and the released hemoglobin in the supernatent was determined from absorbance at 415 nm. Hemolytic activity was determined from the ratio of this absorbance to that of cells that were completely lysed by distilled water.

Kinetic Analyses. Curve fitting of time-dependent fluorescence data was carried out using the program Kaleidograph, using all data points collected for each experiment, and the average of three to five runs. All curves were fit to the single-exponential equation (eq 5).

$$F = F_{inf} + (F_0 - F_{inf}) \exp(-kt) \quad (5)$$

F is the fluorescence at time t; F_0 is the fluorescence at time zero, and F_{inf} is the final, stable intensity. This was based on a first-order process described by the integrated expression for production of C5b-9, $[C5b\text{-}9] = [FITC\text{-}C9]_0 - [FITC\text{-}C9]_0 \exp(-kt)$, and assumed that the fluorescence change reported the fraction of FITC-C9 that was converted to C5b-9. In cases where the fluorescence change did not follow first-order kinetics throughout the entire reaction, the rate constant was estimated from the time to complete 40% of the reaction ($t_{0.4}$) and the relationship $k = \ln(1/0.4)/t_{0.4}$.

RESULTS

Fluorescence Changes Associated with Assembly of FITC-C9. The quantity of FITC-C9 that was capable of assembly with C5b-8 was determined by light scattering measurements as described in Materials and Methods. Full activity was maintained at d:p ratios of up to about 1.0 (Figure 1A). The horizontal and vertical axes show molar equivalents based on protein concentration and protein assembled (assayed by light scattering), respectively. The two independent estimates agree within about 20%. The source of this small error may be derived from measurements of protein and/or phospholipid concentrations.

Assembly of 1 equiv (relative to C5b-7) of FITC-C9 with C5b-8 showed two stages of fluorescence decrease (Figure 1B). Stage 1 was associated with addition of FITC-C9 to C5b-8, a process that resulted in a 19−25% decrease in fluorescence, depending on the level of dye incorporated into the protein. A second decrease of 8−10% (stage 2) occurred upon further addition of unlabeled C9 (Figure 1B). The majority of stage 2 signal change occurred upon addition of 1 equiv of unlabeled C9 (Figure 1B), and the maximum change was obtained with <2 equiv of C9 (data not shown). Thus, more than one process contributed to fluorescence quenching. Assembly of 0.25−1.0 equiv of FITC-C9 per C5b-8 resulted in a relatively constant decrease (25 ± 1%) in steady state fluorescence intensity (Figure 1C) with a small red shift of about 1 nm (Figure 1B). With multiple equivalents of labeled C9, quenching increased to a maximum that was maintained between 6 and 16 FITC-C9 molecules per MAC (Figure 1C). This suggested that a change in the environment of the probe accounted for the fluorescence quenching observed up to 1 equiv of FITC-C9 per MC5b-8. Changes in the fluorescence intensity of fluorescein-labeled proteins associated with binding or conformational transitions have previously been reported (Bock, 1992; Abbott et al., 1991). Further quenching with multiple FITC-C9 molecules may arise from self-energy transfer between the labeled subunits (Sims, 1984). Self-energy transfer accounted for less than half of the total fluorescence quenching. Similar levels of quenching were observed for fluid phase assembly which occurred when FITC-C9 was added to C5b-8 in the absence of membranes (data not shown).

The surface availability of the FITC label on C9 was examined with an antifluorescein antibody. Binding to antifluorescein antibodies can result in greater than 95% fluorescence quenching (Harmer & Samuel, 1989). Antifluorescein antibodies caused 82% quenching of free FITC-C9 fluorescence, 34% quenching of C5b-8−FITC-C9, and

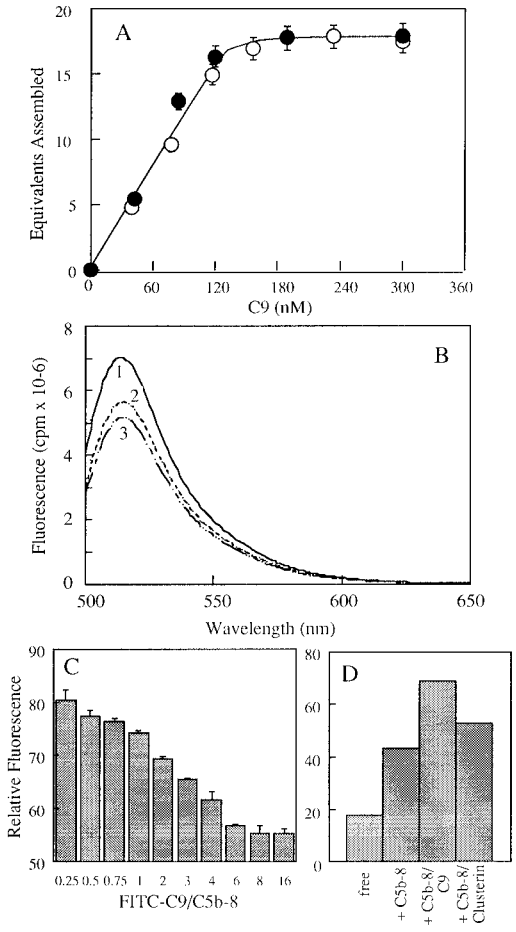

FIGURE 1: Assembly of FITC-C9 and its effect on FITC-C9 fluorescence. (A) Comparison of native and fluorescein-labeled C9. The amounts of C9 shown were added to a previously assembled complex of vesicles (30 μg), C5b-6 (10 nM), C7 (33 nM), and C8 (33 nM) in 0.5 mL of standard buffer. Light scattering intensities from these solutions were used to estimate the amounts of assembled proteins. The experiments shown are for unlabeled C9 (○) and FITC-C9 (d:p = 0.6) (●). Error bars report standard deviations for five measurements. For those measurements that show no error bars, the standard deviation was less than the dimension of the symbol. (B) Emission of FITC-C9 upon assembly in the membrane attack complex. Spectra (excitation at 490 nm) are shown for FITC-C9 (7.5 nM) that was added to solutions containing various mixtures of vesicles (30 μg), C5b-6 (10 nM), C7 (33 nM) and C8 (33 nM). Spectrum 1, unassembled FITC-C9. The reaction mixture, contained all components except C8. Spectrum 2. stage 1 quenching of FITC-C9. The reaction mixture contained all components. Spectrum 3, stage 2 quenching of FITC-C9. The reaction mixture contained all components, and unlabeled C9 (200 nM) was added after the other proteins had assembled. (C) Quenching of FITC-C9 upon assembly of the membrane attack complex. The decrease in fluorescence intensity (excitation at 490 nm, emission at 518 nm) is shown for assembly of various amounts of FITC-C9 (d:p = 1.0) with C5b-8. The amounts of the reagents were as in panel A. The fluorescence intensity is expressed as the percentage of initial signal from unassembled FITC-C9. Error bars report standard deviations of three measurements. (D) Fluorescence quenching induced by antifluorescein antibody. The fluorescence intensity was measured following addition of antifluorescein antibody (2.0 μg) to complexes formed by the their components in 0.5 mL of standard buffer. The relative fluorescence intensity is expressed as a percentage of the intensity of free FITC-C9 (5 nM) in a solution that contained vesicles, C5b-6, C7, and FITC-C9. The amounts of the reagents were as described in panel A. The second column (C5b-8) shows an experiment that contained C8. The third column (C5b-9/C9) showed the result when unlabeled C9 (100 nM) was added to C5b-8−FITC-C9. The fourth column (C5b-8−FITC-C9−clusterin) was the same as the second column but contained clusterin (50 nM).

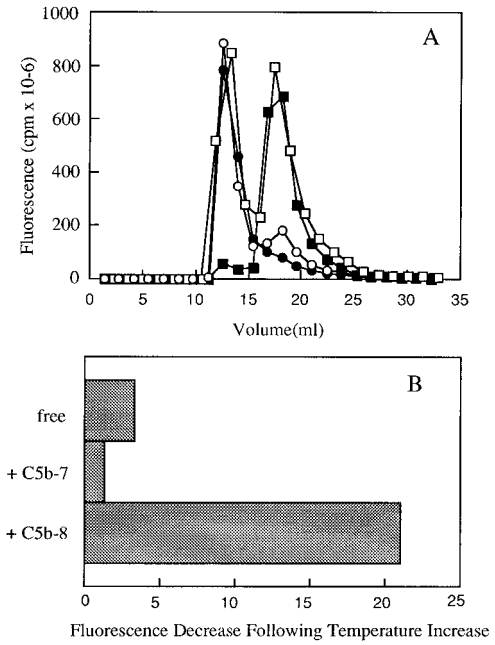

FIGURE 2: Binding of FITC-C9 to the membrane attack complex at low temperatures. (A) Separation of bound and free FITC-C9 by size exclusion chromatography. The fluorescence intensity is shown for 1.9 mL fractions that eluted from a Sephacryl-300 column (29 × 0.9 cm) in standard buffer. Samples (0.5 mL in standard buffer) containing vesicles (115 μg), C5b-6 (150 nM), C7 (50 nM), C8 (150 nM), and FITC-C9 were incubated for 5 min at 0 °C, applied to the column, and eluted at <4 °C. Experiments are shown for mixtures containing FITC-C9 in the following quantities or conditions: 50 nM (○), 100 nM (□); 50 nM preincubated at room temperature for 5 min before loading on column (●); and 50 nM in the absence of C8 (■). Vesicles alone and monomeric C9 eluted at 13 and 18 mL, respectively. (B) Fluorescence decrease of FITC-C9 following a temperature increase. Samples in standard buffer containing vesicles (202 μg/mL), C5b-6 (290 nM), C7 (100 nM), and C8 (0, 270 nM) or buffer alone were loaded into one syringe of the stopped flow, and a solution of FITC-C9 (75 nM) was loaded into the other. The samples were combined, and the mixture was maintained at 0 °C for the first fluorecence intensity measurement. A second measurement was made after the temperature was raised to 25 °C. The percent decrease in fluorescence intensity upon temperature increase is shown. Experiments are shown for FITC-C9 alone (free), in a mixture with all components except C8 (+C5b-7), and in a mixture with all components (+C5b-8).

23% quenching of C5b-8−(FITC-C9−C9 (Figure 1D). It seemed probable that the sites protected from antifluorescein by C5b-8 were involved in stage 1 quenching of FITC-C9, and those protected from antifluorescein antibodies by additional C9 were associated with the quenching produced during stage 2 of C9 assembly.

Binding of FITC-C9 to MAC Complexes. The binding of single equivalents of FITC-C9 to the MAC could be measured by separation of vesicle-associated complexes from free protein by size exclusion chromatography at <4 °C (Figure 2A). A single equivalent of FITC-C9 in a mixture with C5b-7 eluted at the position of the C9 monomer. When chromatographed with C5b-8 that was assembled on vesicles, greater than 80% of the FITC-C9 eluted in the exclusion volume, indicating that it was associated with the vesicles. When the solution was incubated at room temperature for 5 min before chromatography, the remaining fluorescence also shifted to this peak. Incubation of C5b-8 with 2 equiv of FITC-C9 at 0 °C showed equal distribution of FITC-C9 between vesicle-bound and monomeric C9 fractions. This ratio served as an added method for establishing C5b-8 concentrations by the amount of C9 that could be bound without multiple assembly steps. That is, quantitation of C9 equivalents based on the C9:C5b-8 ratio determined by light scattering was consistent with the distribution of fluorescence detected in gel filtration profiles (Figure 2A). The result showed that, at <4 °C, 1 equiv of FITC-C9 was bound to C5b-8 with high affinity but did not undergo the transition necessary for assembly of more C9. This result was consistent with previous reports of high-affinity, reversible binding of 1 equiv of C9 per C5b-8 (MacKay & Dankert, 1994).

In order to relate FITC-C9 binding to C5b-8 at low temperatures with the event that resulted in fluorescence change, FITC-C9 was mixed with C5b-8 and fluorescence was measured before and after a temperature increase. FITC-C9 and the MAC, consisting of either C5b-8 or C5b-7 assembled on SUV, were mixed at 0 °C, and the fluorescence intensity was measured every 5 min. After 15 min, the temperature was increased to 25 °C over a 10 min time period. A new, constant level of fluorescence was achieved. At both temperatures, signal drift was less than 4% over the next 5 min. The temperature increase caused little change in the fluorescence of FITC-C9 alone or in a mixture with C5b-7 (Figure 2B). However, the mixture containing C5b-8 gave a decrease in intensity (22%, Figure 2B) that was equivalent to the change induced by the reaction of FITC-C9 with C5b-8 (Figure 1B,C). These results showed that stage 1 quenching of FITC-C9 did not report initial binding of C9 to C5b-8 but was associated with the irreversible, temperature-dependent transition. This process altered the environment of the probe.

Kinetics of FITC-C9 Fluorescence Quenching. The kinetics of the FITC-C9 fluorescence quenching were used to study the assembly of individual C9 subunits. Fluorescence change, measured in the stopped flow, corresponded to a single-exponential decay (Figure 3A) as analyzed by the curve fitting procedures described in Materials and Methods. The rate constant was independent of the concentration of both FITC-C9 and C5b-8, over a range of 10−200 nM (data not shown). These results were consistent with a mechanism of FITC-C9 activation that consisted of rapid, reversible, high-affinity association with C5b-8 that was followed by a slower conformational transition that gave rise to the fluorescence change as shown below in eq 6:

$$\text{C5b-8} + \text{FITC-C9} \underset{k_{-1}}{\overset{k_1}{\rightleftharpoons}} \text{C5b-8}-\text{FITC-C9} \xrightarrow{k_2} \text{C5b-9} \quad (6)$$

That a simple first-order process was observed under all conditions suggested that $k_2 << k_1$ and [C5b-8] >> k_{-1}/k_1. This method therefore provided an opportunity to study C9 addition reactions. Most previous measurements have been limited to average rates for addition of several C9 molecules.

Arrhenius plots of unimolecular C9 assembly gave an activation energy of 29 kcal/mol (Figure 3B). This was about twice the value obtained in temperature dependence hemolytic studies (13−15 kcal/mol; Lauf, 1975; Li & Levine, 1977), but slightly lower than the value for C9 polymerizarion (37 kcal/mol; Silversmith, 1986a,b). In both cases, the activation energies were based on average velocities over a segment of the complete time course. The rates and activation energy were also measured in the absence of membranes in order to detect possible effects of protein−lipid interactions on C9

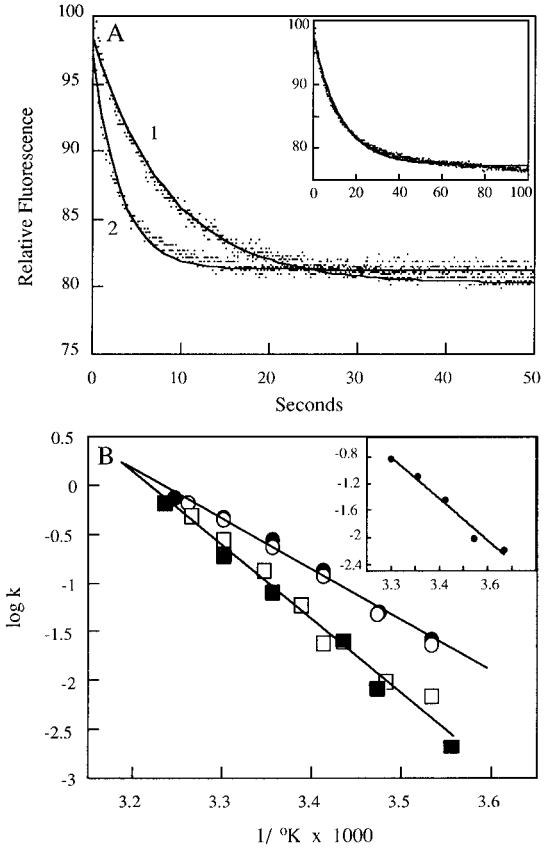

FIGURE 3: Kinetics of FITC-C9 fluorescence change upon assembly with the membrane attack complex. The fluorescence intensity was monitored (excitation at 490 nm, emission at 520 nm) and expressed as a percentage of the fluorescence intensity of free FITC-C9 (200 nM) mixed in buffer. (A) Curve 1, relative fluorescence versus time after mixing of FITC-C9 (150 nM) with previously assembled C5b-8 (vesicles, 460 μg/mL; C5b-6, 200 nM; C7, 400 nM; and C8, 410 nM) in standard buffer. Final concentrations were half of these values. The solid line shows a first-order decay with a rate constant of 0.12 $\pm$ 0.02 s^{-1}. Curve 2, reaction similar to that in curve 1, but with unlabeled C9 (200 nM) added to the complex to produce C5b-9_1. The solid line shows a first-order decay with a rate constant of 0.27 $\pm$ 0.04 s^{-1}. (A, inset) Fluid phase assembly. The reaction was carried out under the conditions described for curve 1, but without membranes. The solid line shows a first-order decay with a rate constant of 0.077 $\pm$ 0.1 s^{-1}. For all curves, the first-order rate constants gave correlation coefficients R of >0.98. (B) Arrhenius plots. Plots are shown for rates of FITC-C9 addition to C5b-8 (□ and ■) as described for curve 1 in panel A and to C5b-9_1 (○ and ●) as described for curve 2 in panel A. A least-squares fit of each plot yielded E_a values of 29 and 21 kcal/mol for FITC-C9 activation by C5b-8 and C5b-9_1, respectively. (B, inset) Rate measurements for FITC-C9 assembly by C5b-8 in the absence of membranes. All other conditions were as described for curve 1 in panel A. The activation energy was 28 kcal/mol.

assembly (Figure 2A, inset). Under these conditions, the activation energy was similar (28 kcal/mol, Figure 3B, inset), indicating that the rate-limiting conformational change was protein-related and uninfluenced by the membrane. A slightly lower rate constant for fluid phase assembly (0.077 $\pm$ 0.008 s^{-1}, Figure 3B, inset) may only be apparent since fluid phase complexes may have some inaccessible C5b-8 sites.

The kinetics of FITC-C9 assembly by C5b-8 and C5b-9_1 were compared (Figure 3A). At 25 °C, the rate constant for FITC-C9 quenching by C5b-8 was about half of that of quenching by C5b-9_1 (Figure 3A). However, the activation energy for C9 activation by C5b-8 was lower (21 kcal/mol,

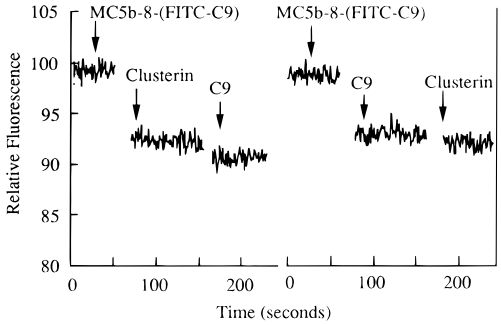

FIGURE 4: Quenching of assembled FITC-C9 by clusterin. The fluorescence intensity was measured (excitation at 490 nm, emission at 520 nm) and shown as a percentage of the initial intensity. The left side of the panel shows the effect of sequential addition of clusterin (31 nM) and unlabeled C9 (150 nM) on the steady state fluorescence of FITC-C9 that was assembled in a C5b-9 complex (vesicles, 50 μg/mL; C5b-6, 20 nM; C7, 34 nM; C8, 25 nM; and FITC-C9, 20 nM in standard buffer), indicated as C5b-8-(FITC-C9). The right side of the panel shows the same experiment with the sequence of clusterin and C9 additions reversed.

Figure 3B). These results suggested that C9 activation on C5b-8 versus C5b-9_1 involved different sites. This could be created by two different sites, one on C5b-8 and the other on C5b-9_1, or by the change of a site on C5b-8 upon addition of the first C9 molecule. An interesting feature of the rates and activation energies was convergence of the actual C9 assembly rate at about 37 °C. Thus, under physiological conditions, C9 assembly would proceed at a constant rate for the first two sites.

Clusterin binding to Assembled FITC-C9. The methods of detecting FITC-C9 assembly allowed for study of the clusterin impact on C9 assembly. Addition of clusterin to a C5b-8−$(FITC\text{-}C9)_1$ complex resulted in a fluorescence decrease that was approximately equal to that caused by addition of unlabeled C9 (compare Figures 4 and 1B). The maximal fluorescence change was reached at approximately a 1:1 ratio of clusterin to C5b-8−$(FITC\text{-}C9)_1$. This indicated a high-affinity binding (data not shown). No decrease in FITC-C9 fluorecence was observed when C8 was omitted or when clusterin was added to free FITC-C9 (data not shown). Addition of unlabeled C9 to the clusterin−C5b-8−$(FITC\text{-}C9)_1$ complex showed slight further quenching, but this did not appear to warrant further study. Previous addition of unlabeled C9 to the C5b-8−$(FITC\text{-}C9)_1$ complex prevented clusterin-induced fluorescence quenching (Figure 4). In addition, clusterin acted in a manner similar to that of unlabeled C9 and protected FITC-C9 from quenching by antifluorescein antibodies (Figure 1D). These results suggested that clusterin and C9 bound to the same site on activated FITC-C9, causing similar levels of fluorescence quenching and providing similar protection of the fluorescence group from antibody binding.

Impact of Clusterin on C9 Assembly. The effect of clusterin on C9 assemby was examined by its influence on the rate of stage 1 fluorescence quenching of FITC-C9. When clusterin was present, the rate of FITC-C9 quenching was reduced (Figure 5A). The degree of the rate reduction was dependent on clusterin concentration (Figure 5A, inset). This behavior suggested reversible competitive binding of clusterin to C5b-8 in a manner that blocked simultaneous association with FITC-C9. The presence of clusterin slowed FITC-C9 assembly to the extent where the end point of the

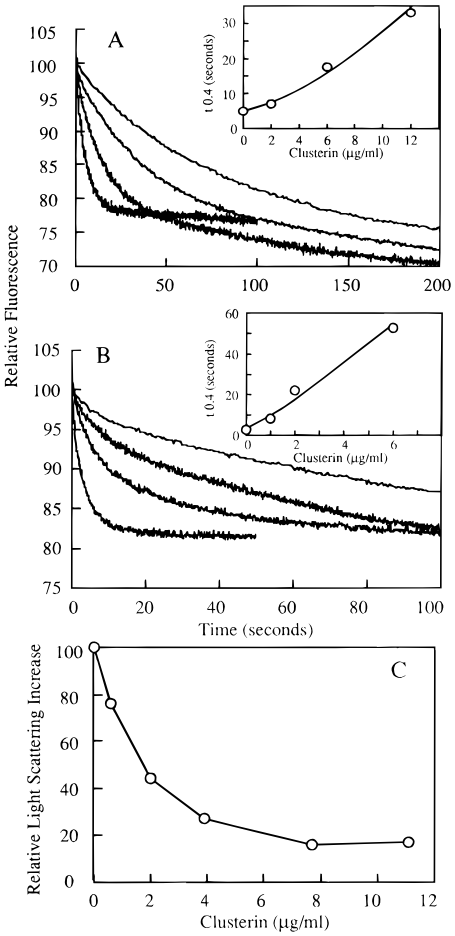

FIGURE 5: Clusterin effect on kinetics of FITC-C9 assembly. (A) Clusterin effect on FITC-C9 addition to C5b-8. A solution of FITC-C9 (50 nM) was rapidly mixed at 25 °C with a solution of C5b-8 (vesicles, 100 μg/mL; C5b-6, 100 nM; C7, 75 nM; and C8, 100 nM) and clusterin in standard buffer. The clusterin concentrations were 0, 50, 150, and 300 nM for the curves from left to right, respectively. Final concentrations were half of these values. (A, inset) Reaction time required to reduce the relative fluorescence to 40% of the maximum change. (B) Clusterin effect on FITC-C9 assembly with C5b-9_1. In standard buffer, FITC-C9 (50 nM) was rapidly mixed with C5b-9_1 (vesicles, 100 μg/mL; C5b-6, 100 nM; C7, 75 nM; C8, 100 nM; and C9, 75 nM) and clusterin. The clusterin concentrations were 0, 25, 50, and 150 nM. Final concentrations were half of these values. (B, inset) Time required to reach 40% of the maximum quenching. (C) Effect of clusterin on C9 polymerization. Light scattering intensity (320 nm excitation, 320 nm emission) was measured following addition of C9 to a complex of C5b-8 (vesicles, 100 μg/mL; C5b-6, 40 nM; C7, 68 nM; and C8, 50 nM) in 0.5 mL of standard buffer at 25 °C in the presence and absence of clusterin. The signal from the C5b-8 complex was I_i. A second intensity measurement (I_f) was made 15 min after the addition of C9 (200 nM). The light scattering increase is shown as a percentage of the increase observed in the absence of clusterin.

reaction was difficult to estimate (Figure 5A). To minimize the effect of variation over long time periods, rate constants were based on $t_{0.4}$ values. The use of longer times would give even greater impacts of clusterin on assembly rates. Clusterin also impacted on rates of FITC-C9 addition to C5b-9_1 (Figure 5B), where its potency was much greater. Once again, the degree of rate reduction was concentration-dependent (Figure 5B, inset). Thus, clusterin appeared to inhibit C9 activation by both C5b-8 and C5b-9_1 by a reversible binding interaction, but possessed a greater affinity for the latter complex.

The rates of C9 addition at the highest concentrations of clusterin were used to estimate the concentration of sites that contained FITC-C9. This estimate assumed that clusterin and C9 were strictly competitive for the same site on the growing polymer, that equilibrium was reached in the time of the assay, and that the rate of the reaction was proportional to the amount of C9 that was reversibly bound to the growth site. The binding events are all of high affinity so that the concentration of free C5b-8 (or C5b-9_1) was negligible. That inhibition increased with clusterin concentration suggested that these assumptions were generally applicable. For interaction of clusterin with C5b-8, the ratio of binding constants can be obtained from eq 9.

$$K_D(\mathrm{CL}) = [\mathrm{CL}]_{free}[\mathrm{C5b\text{-}8}]/[\mathrm{C5b\text{-}8{-}CL}] \quad (7)$$

$$K_D(\mathrm{C9}) = [\mathrm{C9}]_{free}[\mathrm{C5b\text{-}8}]/[\mathrm{C5b\text{-}8{-}C9}] \quad (8)$$

$$K_D(\mathrm{CL})/K_D(\mathrm{C9}) = ([\mathrm{CL}]_{free}/[\mathrm{C9}]_{free})([\mathrm{C5b\text{-}8{-}C9}]/[\mathrm{C5b\text{-}8{-}CL}]) \quad (9)$$

Based on the mechansim of assembly of single C9 molecules described above, its velocity (v) should be described by the equation $v = k_2$[C5b-8−C9]. Reductions in the observed rate constant would therefore correspond to the relative concentration of C5b-8−C9. At 6 μg/mL clusterin (75 nM) and 37.5 nM C5b-8, the rate was reduced to 28% of the maximum so that [C5b-8−C9] = 10.7 nM, $[\mathrm{C9}]_{free}$ = 39 nM, [C5b-8−CL] = 27 nM, and $[\mathrm{CL}]_{free}$ = 48 nM. The ratio of K_D's of clusterin and C9 for C5b-8 was 0.5 so that clusterin displayed twice the affinity of C9. A similar calculation for binding to C5b-9_1 provided that velocity at 75 nM clusterin = 7.2% of the maximum so that [C5b-9_1−C9] = 2.9 nM, [C5b-9_1−CL] = 34.6 nM, $[\mathrm{CL}]_{free}$ = 40 nM, and $[\mathrm{C9}]_{free}$ = 47 nM. The ratio of resulting K_D values was 0.068 so that clusterin bound to C5b-9_1 with 15 times the affinity of C9. Based on the reported K_D of 1 nM for C9 binding to these complexes (MacKay & Dankert, 1994), the K_D values for clusterin would be 0.5 and 0.067 nM for C5b-8 and C5b-9_1, respectively.

The effect of clusterin on C9 polymerization was also examined by light scattering changes following addition of 20 equiv of C9 to C5b-8. Light scattering intensity changes after 15 min were very slow. Clusterin, at concentrations as low as 1 μg/mL, corresponding to less than 0.5 equiv, prevented full polymerizaton within 15 min. However, the highest concentrations did not inhibit polymerization entirely (Figure 5C). These results suggested a potent but reversible mechanism for clusterin inhibition so that irreversible C9 assembly occurred over extended time periods.

Impact of Clusterin on C7 and C8 Assembly. Clusterin inhibition of hemolytic activity has been observed and is proposed to result from clusterin binding to C5b-7, thereby preventing membrane attack by a mechanism similar to that of vitronectin (Murphy et al., 1989a,b). This process was studied by measuring C5b-8-mediated release of dye from carboxyfluorescein-loaded vesicles. The addition of C7 to a mixture of dye-loaded vesicles, C5b-6 (in a limiting amount), and C8 resulted in a rapid fluorescence increase due to release of the dye. The presence of clusterin (8 μg/mL) resulted in a 29 ± 8% inhibition of dye release (Figure 6A). In contrast, clusterin concentrations of up to 15 μg/mL (Figure 6B) appeared to have no impact on C8 assembly.

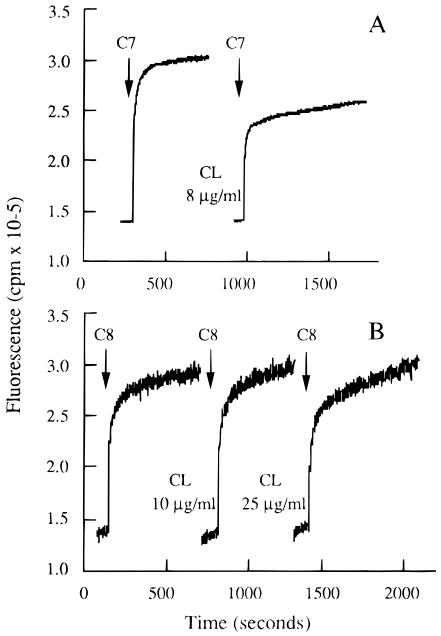

FIGURE 6: Impact of clusterin on C5b-8-induced release of dye from vesicles. Samples contained carboxufluorescein-loaded vesicles (25 μg), C5b-6 (10 nM), C7 (40 nM), and C8 (40 nM) in 1.0 mL of standard buffer at 25 °C. These conditions released 50% of the carboxyfluorescein upon MAC assembly. C7 or C8 was added last (arrows), after incubation of the other components for 5 min. The release of dye from vesicles was detected by its fluorescence intensity (495 nm excitation, 520 nm emission). (A) Clusterin effect on C5b-7 membrane attachment. Experiments show the effect of C7, added as the final component in the absence and presence of clusterin (8 μg/mL, 200 nM). (B) Clusterin effect on C8 assembly with C5b-7. Experiments show the effect of C8, added as the final component in the absence and presence of clusterin (10 μg/mL, 250 nM; 20 μg/mL, 500 nM).

This was examined by adding clusterin to preformed C5b-7−vesicle complexes to which C8 was added to allow dye release. Thus, clusterin inhibited C5b-7 insertion into the membrane and inhibited C9 addition but had no apparent effect on C8 assembly.

DISCUSSION

This investigation described methods that allowed study of individual protein additions to the MAC. The methods were used to determine the interactions of clusterin with the terminal proteins of complement. Clusterin inhibition of complement assembly was derived from three sites and two modes of action. These were related to direct inhibition of C9 assembly at sites on C5b-8 and C5b-9 and to binding to C5b-7 to prevent membrane attachment. The effect on C9 assembly appeared to be the most potent and was derived from reversible binding that reduced the rate of C9 assembly.

A proposed mechanism for C9 assembly and clusterin inhibition is shown in eq 10. The conformational change

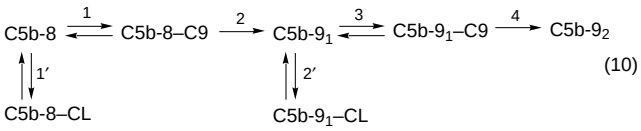

(10)

of C9 that is associated with its irreversible incorporation into the MAC (step 2) conformed to a unimolecular event that occurred subsequent to initial, high-affinity binding (step 1). A two-step assembly agrees with FITC-C9 assembly kinetics (Figure 3A). The kinetic parameters were distinct for activation of FITC-C9 by C5b-8 (0.12 s^{-1}, 29 kcal/mol) versus C5b-9$_1$ (0.27 s^{-1}, 21 kcal/mol), suggesting that C9 activation by these complexes occurred at unique sites. While activation of the first C9 monomer may unmask a new site for binding of the next C9 molecule (step 3), the results did not rule out the possibility that a common site on C5b-8 was used which became modified upon addition of C9. In any case, the difference in activation energies for the two complexes suggests that C9 assembly is site-sensitive. This could be a basis for differences in values that have been reported previously. Earlier studies examined the average of multiple C9 additions; E_a will vary if each assay emphasizes a different stage of polymerization. Another aspect of E_a variation was that different values for C9 polymerization by C5b-8 and C5b-9$_1$ produced a convergence of reaction rates at approximately 37 °C. Thus, even though different sites on C5b-8 and C5b-9 sites may be used, the result under physiological conditions would be homogeneous assembly of C9 for the first 2 equiv. Clusterin inhibition occurred by reversible binding to both C5b-8 (step 1′, eq 10) and C5b-9$_1$ (step 2′) complexes. It displayed about 8-fold greater potency for the C5b-9 complex. This suggested that clusterin interacted with similar but nonidentical sites on C5b-8 versus C5b-9 to block C9 assembly.

Previous studies have reported clusterin binding to C7, the β-subunit of C8, and the C9b−thrombin fragment in their partially denatured forms (Tschopp et al., 1993). While these studies were conducted with nonfunctional (no active MAC) proteins, they appear to be consistent with the general nature of the sites identified in this study. Consequently, the clusterin-binding site on C5b-8 may not be located on the membrane binding domain, which is thought to be associated with the α-subunit of C8, on the basis of labeling by membrane-restricted probes (Steckel et al., 1983). Extension to the current investigation would suggest that the protein−protein contacts reported by FITC-C9 quenching were associated with the extramembrane appendage of C8 and, by extension, of assembled C9. In fact, on the basis of the same criteria as C8$\alpha-\gamma$, the C9b fragment is thought to contain the membrane-binding domain (Ishida et al., 1982). This fragment may be the site of extramembrane protein−protein contacts as well. The finding that the kinetics of FITC-C9 activation were only marginally different for membrane-bound and fluid phase assembly also supported a model in which C9 activation was energetically dominated by protein−protein contacts outside the membrane.

Clusterin binding to C7 (Tschopp et al., 1993) was consistent with its inhibition of C5b-7−membrane attachment found in this study. This presumably occurred by interaction with its membrane-binding domain upon activation by C5b-6. However, the results suggested that the principal source of clusterin inhibiton of complement lysis may be its ability to inhibit C9 assembly. For example, 8 μg of clusterin/mL, a 20-fold excess over C5b-7 so that almost all would be free, was needed to cause a 30% reduction in C5b-7 attachment to vesicles (Figure 6). In contrast, 6 μg/mL total clusterin, corresponding to only a 2-fold excess over C5b-8 so that about 3 μg would be free, caused a 3.5-fold reduction in the rate of C9 activation by C5b-8 (Figure 7A). The same concentration of free clusterin produced a 12-fold reduction in the rate of addition of C9 to C5b-9$_1$ (Figure 5B). The impact of clusterin on the first two steps of C9 addition, at

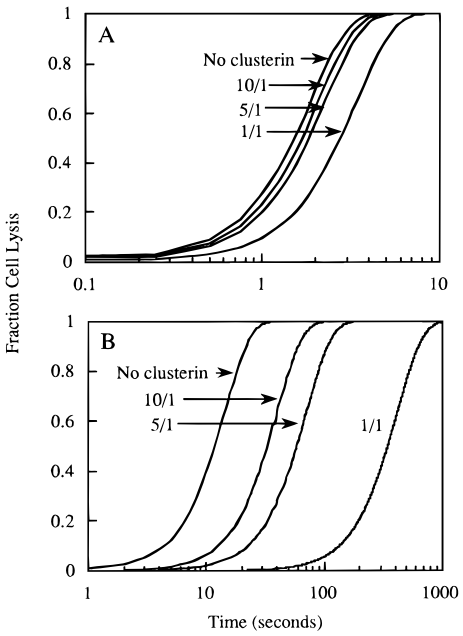

FIGURE 7: Effect of clusterin on the rate of complement-mediated cell killing. The fraction of cells killed was based on the number of cytolytic complexes formed at increasing ratios of clusterin to C9 as described in the Discussion. (A) Clusterin effect on cells that are killed by C5b-9_1. From left to right, lysis curves are shown for C9:clusterin ratios of 0, 10:1, 5:1, and 1:1. Rates of production of C5b-9_1 were 0.12, 0.10, 0.085, and 0.040 s^{-1}, respectively. (B) Clusterin effect on cells that are killed by C5b-9_3. Lysis curves are shown for the same clusterin:C9 ratios as in panel A. Rates of production of C5b-9_3 were 87.5×10^{-4}, 12.1×10^{-4}, 3.9×10^{-4}, and 0.12×10^{-4} s^{-1}, respectively.

the concentration of components used in Figure 6, would result in a 40-fold reduction in the rate at which C5b-9_2 would be formed.

The relative rate of C9 addition at higher concentrations of C9 can be estimated using the ratio of K_D values obtained in eq 7. At plasma concentrations of C9 (0.75 μM), a free concentration of clusterin of 66 nM (about 5% of total clusterin) would reduce the rate of C9 addition to C5b-8 to 85% of the maximum. However, it would reduce the rate of C9 addition to C5b-9_1 by more than half. The rate of forming a C5b-9_3 polymer would be reduced by the product of three steps ($0.85 \times 0.43 \times 0.43$), to give an overall rate for C5b-9_3 formation which was 16% of that in the absence of clusterin. This is much greater than the impact of clusterin on C5b-7 interaction with the membrane (100 nM reduced vesicle lysis by only 30%, Figure 6). The impact of clusterin will therefore depend on the relative concentrations of C9 and clusterin. If they are present in equimolar quantities, which may occur in those conditions where clusterin is most abundant, the rate of formation of C5b-9_3 would be reduced to 0.1% of its maximum. Thus, studies which concentrate on the ability of clusterin to block hemolysis of erythrocytes may underestimate its impact since a single subunit of C9 is sufficient for erythrocyte lysis. Cells that require higher levels of C9, including most nucleated cells, would receive much greater protection by clusterin.

In order to illustrate this behavior, the time required for lysis of cells that required production of C5b-9_1 or C5b-9_3 was estimated. The rate constants for production of C5b-9_1 (activation of C9 by C5b-8) were calculated for various C9:clusterin ratios and the ratio of K_D's provided by eq 7. For production of C5b-9_3, the rate constants for addition to C5b-8 were multiplied by the square of the rate constants for activation of C9 by C5b-9_1, in the presence of the same amount of clusterin. The number of cytolytic complexes (CyC), either C5b-9_1 or C5b-9_3, was determined from the relationship $[CyC]_t = [CyC]_{t-1} + kt(1 - [CyC]_{t-1})$. The inital concentration of the precursor complex (C5b-8) was 1 per cell. The half-time for cell death from a C5b-9_1 complex (e.g. erythrocyte lysis) would be reduced by only about 15% at a clusterin:C9 ratio of 1:10 and by 67% at 1:1 (Figure 7A). This appeared to agree with studies showing that 5−50 μg/mL clusterin reduced erythrocyte hemolysis by 25−80%, depending on the concentration of C5b-8 (Murphy et al., 1989a,b). Thus, for preventing lysis of red cells, clusterin binding to C5b-7 may play the larger role. However, if C5b-9_3 were required for cell killing, a clusterin:C9 ratio of 1:10 would reduce the rate of cell killing by 8-fold, and at 1:1 by 100-fold (Figure 7B). The 1:10 ratio corresponds to about 10% of the circulating clusterin (50−300 μg/mL) and all of the circulating C9 (approximately 50 μg/mL).

Most of the clusterin may be found in circulating complexes with apolipoprotein A-1 (Jenne et al., 1991), vitronectin (Murphy et al., 1988), and even amyloid β peptides (Ghiso et al., 1993), so the ability to exchange clusterin from these sites would impact MAC assembly. Some other circumstances provide high clusterin. For example, clusterin is found at 10-fold higher concentrations in seminal plasma (Murphy et al., 1989a,b) and in blood plasma from pathological states. In the latter, it is thought to serve multiple roles, including clearance and tissue repair (Rosenberg & Silkensen, 1995). The effects of clusterin would be superimposed on other complement resistance pathways, such as blebbing (Campbell & Morgan, 1985; Toney & Marciano-Cabral, 1994) and membrane-associated inhibitors (Meri et al., 1990; Hefferman et al., 1992). If the rate of blebbing, or pinching off extracellular vesicles, were lower than the rate of C9 assembly, clusterin could greatly enhance complement resistance by the blebbing process.

Overall, clusterin inhibition of complement can be a major contributor to protection of host cells from complement destruction, especially in some tissues and physiological states. The high affinity of the clusterin−MAC interaction suggests important biological functions that may be more evident with further study.

REFERENCES

Abbott, A. J., Amler, E., & Ball, W. J., Jr. (1991) *Biochemistry 30*, 1692.
Biesecker, G., & Mueller-Eberhard, H. J. (1980) *J. Immunol. 124*, 1291.
Bloomfield, V. A., & Lim, T. K. (1978) *Methods Enzymol. 48*, 415.
Bock, P. E. (1992) *J. Biol. Chem. 267*, 14974.
Bradford, M. M. (1976) *Anal. Biochem. 72*, 248.
Campbell, A. K., & Morgan, B. P. (1985) *Nature 317*, 164.
Chen, P. S., Toribara, T. Y., & Warner, H. (1956) *Anal. Chem. 28*, 7005.
Ghiso, J., Matsubara, E., Koudinov, A., Choi-miura, N. H., Tomita, M., Wisniewski, T., & Frangione, B. (1993) *Biochem. J. 293*, 27.
Harmer, I. J., & Samuel, D. (1989) *J. Immunol. Methods 122*, 115.
Haugland, R. P. (1992) *Handbook of Fluorescent Probes and Research Chemicals*, p 22, Molecular Probes, Eugene, OR.
Hefferman, E. J., Reed, S., Hackett, J., Fierer, J., Roundier, C., & Guiney, D. (1992) *J. Clin. Invest. 90*, 953.
Ishida, B., Wisnieski, B. J., Lavine, C. H., & Esser, A. F. (1982) *J. Biol. Chem. 257*, 10551.

Jenne, D. E., Lowin, B., Peitsch, M. C., Bottcher, A., Schmitz, G., & Tschopp, J. (1991) *J. Biol. Chem. 266*, 11030.
Kabat, E. A., & Mayer, M. M. (1961) *Experimental Immunochemistry*, p 149, Charles C. Thomas Ltd., Springfield, IL.
Kirszbaum, L., Sharpe, J. A., Murphy, B., d'Apice, A. J. F., Classon, B., Hudson, P., & Walker, I. D. (1989) *EMBO J. 8*, 711.
Laemmli, U. K. (1970) *Nature 227*, 680.
Lauf, P. K. (1975) *J. Exp. Med. 142*, 947.
Li, C. K. N., & Levine, R. P. (1977) *Immunochemistry 14*, 421.
MacKay, S. L. D., & Dankert, J. R. (1994) *Infect. Immun. 62*, 2800.
Meri, S., Morgan, B. P., Davies, A., Daniels, R. H., Olaveson, M. G., Waldmann, H., & Lachmann, P. J. (1990) *Immunology 71*, 1.
Murphy, B. F., Kirszbaum, L., Walker, I. D., & d'Apice, A. J. F. (1988) *J. Clin. Invest. 81*, 1858.
Murphy, B. F., Kirszbaum, L., Morrow, W., & d'Apice, A. J. (1989) *Pathology 21*, 275.
Murphy, B. F., Saunders, J. R., O'Bryan, M. K., Kirszbaum, L., Walker, I., & d'Apice, A. J. F. (1989b) *Int. Immunol. 1*, 551.
Nelsestuen, G. L., & Lim, T. K. (1977) *Biochemistry 16*, 4164.
Plager, D. A., & Nelsestuen, G. L. (1994) *Biochemistry 33*, 7005.
Podack, E., Kolb, W., & Muller-Eberhard, H. J. (1978) *J. Immunol. 120*, 1841.
Podack, E., Kolb, W., Esser, A., & Muller-Eberhard, H. J. (1979) *J. Immunol. 123*, 1071.
Podack, E. R., & Tschopp, J. (1982) *Proc. Natl. Acad. Sci. U.S.A. 79*, 574.
Podack, E. R., & Tschopp, J. (1984) *Mol. Immunol. 21*, 589.
Rosenberg, M. E., & Silkensen, J. (1995) *Int. J. Biochem. Cell Biol. 27*, 633.
Rosenberg, M. E., Dvergsten, J., & Correa-Rotter, R. (1993) *J. Lab. Clin. Med. 121*, 205.
Silkenson, J. R., Skubitz, K. M., Skubitz, A. P., Chmielewski, D. H., Manivel, J. C., Dvergsten, J. A., & Rosenberg, M. E. (1995) *J. Clin. Invest. 96*, 2646.
Silversmith, R. E., & Nelsestuen, G. L. (1986a) *Biochemistry 25*, 841.
Silversmith, R. E., & Nelsestuen, G. L. (1986b) *Biochemistry 25*, 852.
Silversmith, R. E., & Nelsestuen, G. L. (1986c) *Biochemistry 25*, 7717.
Sims, P. J. (1984) *Biochemistry 23*, 3248.
Smith, P. K., Krohn, R. I., Hermanson, G. T., Mallia, A. K., Gartner, F. H., Provenzano, M. D., Fujimoto, E. K., Goeke, N. M., Olson, B. J., & Klenk, D. C. (1985) *Anal. Biochem. 150*, 76.
Stanley, K. K., & Herz, J. (1987) *EMBO J. 6*, 1951.
Steckel, E. W., York, R. G., Monahan, J. B., & Sodetz, J. M. (1980) *J. Biol. Chem. 255*, 11997.
Steckel, E. W., Welbaum, B. E., & Sodetz, J. M. (1983) *J. Biol. Chem. 258*, 4318.
Toney, D. M., & Marciano-Cabral, F. (1994) *J. Immunol. 152*, 2952.
Tschopp, J., Chonn, A., Hertig, S., & French, L. E. (1993) *J. Immunol. 151*, 2159.
Vakeva, A., Laurila, P., & Meri, S. (1993) *Immunology 80*, 182.

BI962895R